Neutrophil Transepithelial Migration: Evidence for Sequential, Contact-Dependent Signaling Events and Enhanced Paracellular Permeability Independent of Transjunctional Migration[1]

Heather A. Edens,[2]* Boaz P. Levi,* David L. Jaye,* Shaun Walsh,* Titus A. Reaves,* Jerrold R. Turner,† Asma Nusrat,* and Charles A. Parkos*

Active migration of polymorphonuclear leukocytes (PMN) through the intestinal crypt epithelium is a hallmark of inflammatory bowel disease and correlates with patient symptoms. Previous in vitro studies have shown that PMN transepithelial migration results in increased epithelial permeability. In this study, we modeled PMN transepithelial migration across T84 monolayers and demonstrated that enhanced paracellular permeability to small solutes occurred in the absence of transepithelial migration but required both PMN contact with the epithelial cell basolateral membrane and a transepithelial chemotactic gradient. Early events that occurred before PMN entering the paracellular space included increased permeability to small solutes (<500 Da), enhanced phosphorylation of regulatory myosin L chain, and other as yet undefined proteins at the level of the tight junction. No redistribution or loss of tight junction proteins was detected in these monolayers. Late events, occurring during actual PMN transepithelial migration, included redistribution of epithelial serine-phosphorylated proteins from the cytoplasm to the nucleus in cells adjacent to migrating PMN. Changes in phosphorylation of multiple proteins were observed in whole cell lysates prepared from PMN-stimulated epithelial cells. We propose that regulation of PMN transepithelial migration is mediated, in part, by sequential signaling events between migrating PMN and the epithelium. ***The Journal of Immunology*****, 2002, 169: 476–486.**

The tight junction (TJ),[3] an intercellular junction at the most apical region of the lateral membrane in polarized epithelia and endothelia, acts as the rate-limiting step in the paracellular pathway for ions and larger solutes and controls cell membrane polarity (1–3). The TJ plays an important role in the migration of immune cells across the paracellular space during inflammation and immune surveillance (4, 5). Altered intestinal epithelial paracellular permeability has been implicated as an important pathogenic factor in active migration of polymorphonuclear leukocytes (PMN) through the intestinal crypt epithelium, a key feature of idiopathic inflammatory bowel disease, Crohn's disease, and ulcerative colitis (6, 7). Many of the symptoms of these disorders can be attributed to disruption in the epithelial barrier that acts in a protective capacity by restricting the access of lumenal microbes and harmful substances to the underlying tissue.

The TJ undergoes dynamic physiological changes when stimulated by various mediators, such as cytokines (8, 9) and microbial toxins (10, 11). Multiple second messenger pathways have been found to modulate permeability characteristics of developing and mature junctions by modification of various junctional proteins' phosphorylation state and/or linkage to the actin cytoskeleton (9, 12–15). Furthermore, actin-myosin interactions, promoted by phosphorylation of the 20-kDa regulatory myosin L chain (MLC), control the contractility of actomyosin in nonmuscle cells (16). Agents that stimulate contraction of the actomyosin ring cause a decrease in barrier function (enhanced paracellular permeability), while relaxation results in enhanced barrier function (decreased paracellular permeability) (17).

In previous work, our laboratory has shown that high-density PMN migration across model epithelial monolayers in vitro results in the disruption of epithelial permeability (18–20) and the production of multifocal wounds in the epithelia that are able to reseal following removal of PMN (18, 21). Alternatively, in vitro studies using Madin-Darby canine kidney (22) or T84 cells (18), a model human intestinal epithelial cell line, demonstrate that barrier function is preserved during low-density PMN transepithelial migration, suggesting that the opening of the intercellular junctions is a rapid and reversible process. Indeed, passage of migrating immune cells across vascular endothelium or epithelial monolayers, during a normal immune response or immune surveillance, is generally believed to be a rapid process that does not damage the integrity of the monolayer. Therefore, transcellular migration requires mechanisms that open intercellular junctions to allow passage of circulating cells while, at the same time, maintaining barrier function. However, the mechanisms that govern this process remain undefined.

*Division of Gastrointestinal Pathology, Department of Pathology and Laboratory Medicine, Emory University, Atlanta, GA 30322; and †Department of Pathology, University of Chicago, Chicago, IL 60637

Received for publication February 12, 2002. Accepted for publication May 1, 2002.

The costs of publication of this article were defrayed in part by the payment of page charges. This article must therefore be hereby marked *advertisement* in accordance with 18 U.S.C. Section 1734 solely to indicate this fact.

[1] This work was supported by grant awards from the Crohn's and Colitis Foundation of America and National Institutes of Health Grants DK61264-01 (to H.A.E.), DK 6137919, HL60540, and HL54299 (to C.A.P.), DK53202 (to A.N.), and R01DK61931 (to J.R.T.).

[2] Address correspondence and reprint requests to Dr. Heather A. Edens, Division of Gastrointestinal Pathology, Department of Pathology and Laboratory Medicine, Emory University, 615 Michael Street, Whitehead Building, Room 123D, Atlanta, GA 30322. E-mail address: hedens@emory.edu

[3] Abbreviations used in this paper: TJ, tight junction; AJ, adherens junction; PMN, polymorphonuclear leukocyte; TER, transepithelial electrical resistance; BCECF-AM, 2′,7′-bis-(2-carboxyethyl)-5-(and-6)-carboxyfluorescein, acetoxymethyl ester; MLC, myosin L chain; pMLC, phosphorylated MLC; MLCK, MLC kinase.

0022-1767/02/$02.00

In this study, using a physiologically relevant model of PMN transepithelial migration in which PMN migrate in the basolateral to apical direction, we have characterized PMN-induced alterations in T84 monolayers that occur in a step-wise fashion during PMN migration. This is the first report demonstrating that PMN-induced changes in epithelial biology occur at both early and later stages of the transepithelial migration process. Early events, defined as those that occurred before PMN entering the paracellular space, included enhanced epithelial permeability, increased phosphorylation of MLC at the actomyosin ring, and other proteins at the TJ. Later events occurring as PMN migrate through the paracellular space were characterized by the relocalization of phosphoserine proteins from the cytoplasm to the nucleus in epithelial cells directly adjacent to migrating PMN. These findings are discussed in the context of the regulation of PMN transepithelial migration during physiological and pathophysiological processes.

Materials and Methods

Antibodies

All Abs used in this study are listed in Table I.

Cell culture

Stock cultures of T84 epithelial cell monolayers were grown as previously described (23). For PMN transmigration experiments, T84 monolayers were grown on 0.33-cm^2 permeable supports with pores of 5 or 0.4 μm in diameter (Costar, Cambridge, MA) as either standard or inverted monolayers (Fig. 1*A*) as previously described (23, 24). Confluence and TJ maturation were determined by monitoring the transepithelial electrical resistance (TER) to passive ion flow and were used when resistances had reached $\geq$800 $\Omega \cdot cm^2$, generally 1500–2000 $\Omega \cdot cm^2$, ~6–10 days postseeding (25).

PMN isolation

Normal human PMN were isolated from noncoagulated citrated blood by Ficoll-Paque (Amersham Pharmacia Biotech, Uppsala, Sweden) density sedimentation as per the manufacturer's instructions. PMN were suspended in modified HBSS (Sigma-Aldrich, St. Louis, MO) containing 0.4 g/L KCl, 0.06 g/L KH_2PO_4, 8 g/L NaCl, 0.048 g/L Na_2HPO_4, 0.01 g/L glucose, and 10 mM HEPES (pH 7.4) at 4°C. For all transmigration experiments, PMN were suspended in HBSS containing 0.185 g/L $CaCl_2$ and 0.098 g/L $MgSO_4$. For some transmigration assays that were further evaluated by immunofluorescence microscopy, PMN were loaded with the fluorochrome 2′,7′-bis-(2-carboxyethyl)-5-(and-6)-carboxyfluorescein, acetoxymethyl ester (BCECF-AM; Molecular Probes, Eugene, OR) as per the manufacturer's instructions.

PMN transepithelial migration

PMN transmigration experiments were performed with standard or inverted T84 monolayers as previously described in detail (23) (Fig. 1*A*). Briefly, the upper reservoir was filled with 150 μl of HBSS with or without Abs, or 10^{-6} M fMLP in HBSS followed by the addition of PMN to the upper well (10^6 or 2×10^6 total PMN per inverted or standard monolayers, respectively). Monolayers were then transferred to wells containing HBSS or 10^{-6} M fMLP ($t = 0$) and incubated for the indicated time at 37°C. PMN that had migrated through the monolayer and into the lower reservoir, or PMN found within the monolayer and filter, were quantified by assaying for myeloperoxidase (23).

Microscopy

After a defined period of PMN transepithelial migration, T84 monolayers were washed with ice-cold HBSS. Non- or semiadherent PMN were removed by gentle washing with care taken to avoid disturbing the filter or T84 monolayer. For immunofluorescence analysis, monolayers were fixed with 10% neutral buffered formalin (Sigma-Aldrich) for 10 min at room temperature followed by treatment with 4 mg/ml sodium borohydride for 30 min to 1 h at 4°C. Monolayers were then permeabilized with 0.2% saponin (Sigma-Aldrich) in 1% BSA. Samples were incubated with primary Abs overnight at 4°C and then probed with secondary Abs coupled with Alexa-488 (Molecular Probes), Alexa-568 (1:1000), or Cy5 (1:500) (Jackson ImmunoResearch Laboratories, West Grove, PA) for 1 h at room temperature. Cells were stained with rhodamine-phalloidin (1:1000; Molecular Probes) to visualize F-actin, or propidium iodide (1 μg/ml; Molecular Probes) to visualize the nuclei. Stained monolayers were mounted in Slow Fade medium (Molecular Probes) and examined using a Zeiss 510 confocal microscope (Zeiss, Oberkochen, Germany).

For light microscopy, samples were fixed with 4% buffered glutaraldehyde, postfixed in 1% osmium tetraoxide, dehydrated, and embedded. Semithin (500 nm) sections were stained with toluidine blue and examined by light microscopy.

Table I. *Antibodies*

Ag	Ab or Catalog No.	Host	Immunofluorescence Concentration	Western Blot Concentration	Source
Actin	A2668	Rabbit IgG	ND[a]	1/500	Sigma-Aldrich
α-Catenin	C21620/L2	Mouse IgG1	ND	1/250	BD Transduction Laboratories (Franklin Lakes, NJ)
β-Catenin	C19220/L4	Mouse IgG1	1/500	1/1000	BD Transduction Laboratories
γ-Catenin	C26220/L4	Mouse IgG2a	1/250	1/2000	BD Transduction Laboratories
Claudin-1	71–7800	Rabbit IgG	1/100	1/250	Zymed Laboratories (San Francisco, CA)
E-cadherin	13–1700	Mouse IgG1	10 μg/ml	ND	Zymed Laboratories
MHC class I[b]	W6/32	Mouse IgG1	ND	ND	Purified from ascities
MLC	M-4401	Mouse IgM	1/200	1/2000	Sigma-Aldrich
MLC	sc-9449	Goat IgG	ND	1/4000	Santa Cruz Biotechnology (Santa Cruz, CA)
pMLC	Serum	Rabbit IgG	ND	1/1000	Dr. J. Turner (University of Chicago, Chicago, IL)[c]
pMLC	sc-12896	Goat IgG	1/100	ND	Santa Cruz Biotechnology
Occludin	71–1500	Rabbit IgG	1/400	1/1000	Zymed Laboratories
Phosphoserine	61–8100	Rabbit IgG	1/100	1/1000	Zymed Laboratories
Phosphothreonine	71–8200	Rabbit IgG	1/100	1/1000	Zymed Laboratories
Phosphotyrosine	4G10	Mouse IgG2b	5 μg/ml	1/4000	Upstate Biotechnology (Lake Placid, NY)
Phosphotyrosine	13–6600	Mouse IgG1, IgG3, IgG2b	1/100	1/1000	Zymed Laboratories
ZO-1	61–7300	Rabbit IgG	1/400	1/500	Zymed Laboratories

[a] ND, Not done.
[b] W6/32 used as an isotype-matched, binding control Ab for PMN transepithelial migration assays.
[c] Ref. 54.

Western blot analysis

Urea-glycerol gel electrophoresis was conducted on monolayers to analyze myosin L chain phosphorylation as performed by Garcia et al. (26) and isa modified method of Persechini et al. (27) and Verin et al. (28). T84 cells were scraped off the filter into HBSS containing protease and phosphatase inhibitors (10 μl/ml protease inhibitor mixture; catalog no. P8340, Sigma-Aldrich), 0.2 mM PMSF, 1 mM sodium fluoride, and 1 mM sodium orthovanadate at 4°C. Protein was precipitated with trichoroacetic acid (10% v/v) and 10 mM DTT for 30 min at 4°C, followed by pelleting in a microcentrifuge. The protein pellet was then washed with acetone, air-dried, and suspended in urea sample buffer, in which 15 μl of sample buffer was used per protein pellet from a single 0.33-cm^2 monolayer. Equal protein amounts were run out on a native protein gel, transferred to nitrocellulose, and then analyzed by Western blot. The nitrocellulose was blocked with 3% BSA and probed with anti-MLC Ab followed by HRP-conjugated secondary Ab (Jackson ImmunoResearch Laboratories) and ECL to visualize the bands (Amersham Pharmacia Biotech). Band intensity was quantitated using the Chemi Image 5500, software version 3.4C (Alpha Innotech, San Leandro, CA).

For general analysis of protein phosphorylation (tyrosine, serine, and threonine), whole cell lysates of T84 monolayers were prepared following interaction of PMN with T84 monolayers for the specified amount of time. T84 monolayers were washed free of adherent PMN and scraped into lysis buffer containing 8 M urea and 1% SDS followed by boiling for 10 min.

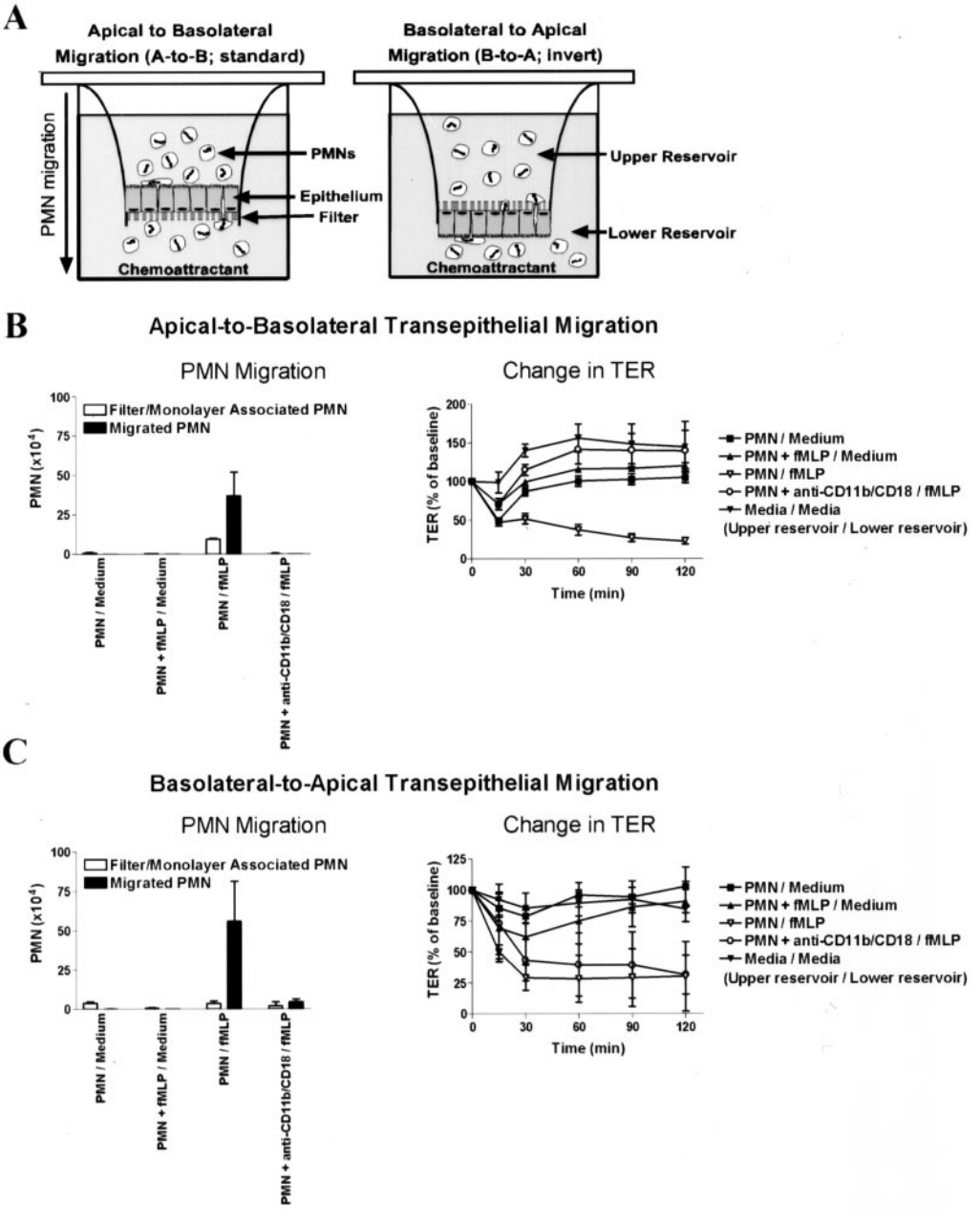

FIGURE 1. PMN stimulate a decrease in T84 monolayer barrier function in the basolateral to apical direction that is independent of transmigration. *A*, In vitro assay of PMN-epithelia interactions. PMN migrate through the T84 epithelial monolayer toward the chemoattractant, fMLP (1 μM), in the lower reservoir in either the apical to basolateral direction (*left schematic*) or the basolateral to apical direction (*right schematic*). *B*, Apical to basolateral PMN transepithelial migration. After 2 h, migrated PMN were quantitated in both the lower reservoir (filled bars) and those that remained associated with the monolayer and filter (open bars), as described in *Materials and Methods*. TER was monitored at specified time points during PMN transmigration and is plotted as the percentage of the baseline TER ($t = 0$ h). PMN migration was inhibited by the addition of anti-CD11b/CD18 to the upper reservoir along with PMN. *C*, Basolateral to apical PMN transepithelial migration. PMN migration was quantified the same as in *B* and the change in T84 monolayer TER was monitored the same as in *B*. Values in *B* and *C* are the average ± SD from a single representative experiment performed in triplicate.

Samples were mixed with Laemmli sample buffer and equal amounts of protein were separated on 4–20% SDS PAGE (Bio-Rad, Chicago, IL). Proteins were transferred to nitrocellulose and probed with anti-phosphoprotein Abs (listed in Table I) diluted in 3% BSA/TBS overnight at 4°C followed by HRP-conjugated secondary Ab and ECL.

FITC-dextran and mannitol permeability assays

Permeability was assessed by determining the flux of FITC-dextran (m.w., 3000; Molecular Probes) or [^{14}C]mannitol (ICN Pharmaceuticals, Costa Mesa, CA) across T84 monolayers by passive diffusion in the basolateral to apical direction across the paracellular space as previously described (29, 30). A Beckman LS6000SC (Beckman Coulter, Fullerton, CA) was used for liquid scintillation counting and a Cytofluor Fluorescence Multiplate Reader (Applied Biosystems, Foster City, CA) was used for measuring fluorescence intensity.

Results

Increased paracellular permeability in T84 monolayers is stimulated by subepithelial PMN and occurs independent of transepithelial migration

The results of PMN transepithelial migration assays across T84 monolayers in the apical to basolateral direction and the physiologically relevant basolateral to apical direction toward a gradient of fMLP are shown in Fig. 1. Independent of the direction of PMN transepithelial migration, each sample is defined by the conditions of the upper and lower reservoirs as upper reservoir/lower reservoir (see Fig. 1*A*). For example, a sample with PMN added to the upper reservoir and fMLP added to the lower reservoir would be listed as PMN/fMLP. As we have previously shown, robust PMN migration occurred toward fMLP (PMN/fMLP) in both directions, with the majority of migrating PMN found in the lower reservoir (Fig. 1, *B* and *C*, filled bars) and a small component of PMN remaining in the monolayer and filter (Fig. 1, *B* and *C*, open bars). PMN transmigration in the apical to basolateral direction induced a decrease in TER, a measure of paracellular permeability, to ~30% of the baseline resistance after 60 min (PMN were added to the monolayer at $t = 0$ h) and correlated with PMN migration into the lower chamber (Fig. 1*B*; compare PMN migration with the change in TER). The addition of inhibitory anti-β_2 integrin Abs, CD11b/CD18, to the upper reservoir completely blocked PMN migration in the apical to basolateral direction and the corresponding decrease in TER, as we have previously shown (20, 23). Furthermore, no decrease in TER was observed when PMN were added to the upper reservoir without a chemotactic gradient (PMN/medium) or when fMLP was added to the upper reservoir together with PMN (PMN + fMLP/medium).

Strikingly, a distinctly different TER response was seen when PMN migration in the basolateral to apical direction was inhibited by the addition of anti-CD11b/CD18 Abs (Fig. 1*C*). While PMN migration in the basolateral to apical direction was inhibited 89% by anti-CD11b/CD18 Abs, a decrease in TER occurred similar to that observed for uninhibited migration in either direction (Fig. 1, compare *B* and *C*, PMN/fMLP). Thus, marked inhibition of transepithelial migration in the basolateral to apical direction still resulted in a decrease in TER similar to that of uninhibited controls. These results suggest that PMN applied to the basolateral surface of T84 monolayers in the presence of a chemotactic gradient cause an increase in epithelial permeability that is independent of transepithelial migration.

PMN-induced decrease in epithelial monolayer TER does not correlate with migration

While anti-CD11b/CD18 Abs inhibited the majority of PMN transepithelial migration, a small amount of migration occurred in the basolateral to apical direction. Thus, experiments were designed to test whether a small number of migrating PMN could cause a large decrease in TER (Fig. 2). As shown for both conditions, increasing concentrations of fMLP or PMN resulted in a decrease in TER that correlated with increasing numbers of migrating PMN (uninhibited migration). Yet, when anti-CD11b/CD18 Abs were used to inhibit PMN migration, the decrease in TER was far greater than samples with the same or significantly greater amounts of migrating PMN. These results indicate that the decrease in TER does not correlate with PMN migration in the basolateral to apical direction and suggest that PMN stimulate a change in barrier function when applied to the basolateral surface of epithelial monolayers in the presence of a transepithelial chemotactic gradient.

Experiments were also performed with T84 monolayers cultured on permeable supports with pores too small to permit the passage of PMN (0.4 μm in diameter). Both morphologic assessment and myeloperoxidase assays confirmed that PMN applied to the upper reservoir (the basolateral aspect of the epithelial monolayer) were unable to migrate across the monolayer (data not shown). When this modified system was used to evaluate the kinetics of the TER decrease after basolateral application of PMN, a drop in TER was observed with the application of a transepithelial gradient of fMLP (Fig. 3*A*). Similar results were obtained using anti-CD11b/CD18 Abs (data not shown). In comparison to the assay using T84 monolayers cultured on 5-μm pore filters (Fig. 1*C*), the time course of

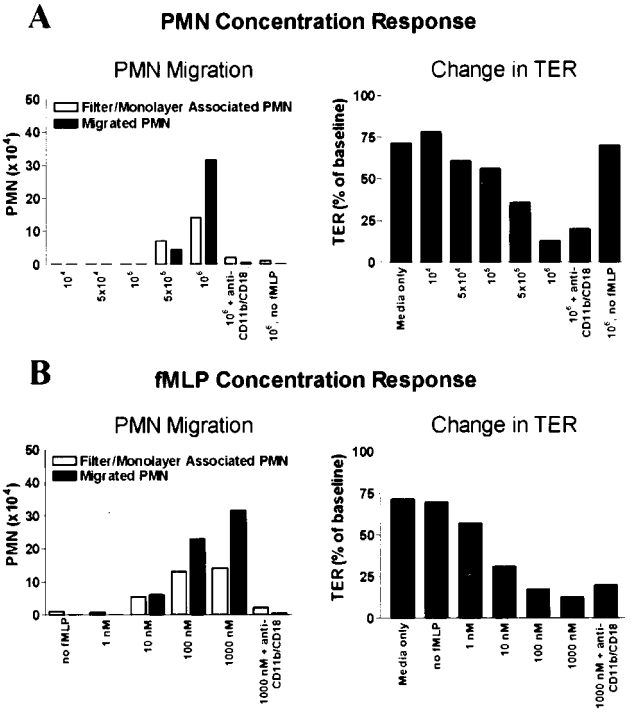

FIGURE 2. PMN-induced decrease in epithelial monolayer TER does not correlate with migration. *A*, Increasing concentrations of PMN (10^4–10^6 cells) were added to the basolateral aspect of T84 monolayers and induced to migrate in the basolateral to apical direction toward a gradient of fMLP (10^{-6} M) in the lower reservoir. *B*, PMN (10^6 cells) were added to the basolateral aspect of T84 monolayers and induced to migrate across T84 monolayers in the basolateral to apical direction toward increasing concentrations of fMLP (1–1000 nM) in the lower reservoir. Negative control, no fMLP; positive control, inhibition of migration by anti-CD11b/CD18 Abs. After 2 h, PMN were quantitated in both the lower reservoir (filled bars) and those that remained associated with the monolayer and filter (open bars) as described in *Materials and Methods* (*left panels*). TER was determined for the same monolayers after 2 h of PMN migration and is plotted as the percentage of the baseline TER at $t = 0$ h (*right panels*). Values are the average of duplicate samples and are from one of three experiments performed.

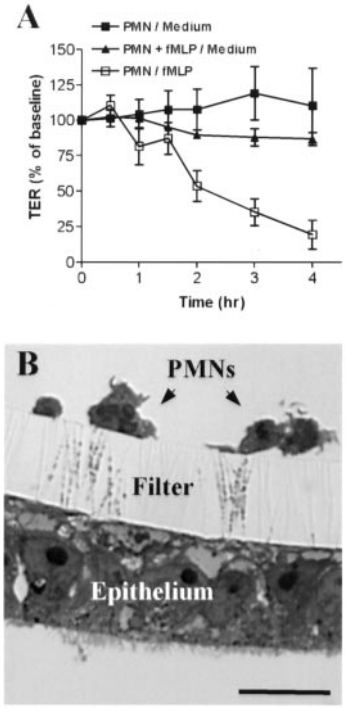

FIGURE 3. PMN stimulate a decrease in TER in epithelial monolayers cultured on 0.4-μm pore filters and are able to contact the monolayer across the filter. *A*, PMN were added to the basolateral aspect of inverted T84 monolayers cultured on 0.4-μm pore filters. TER was monitored at specified time points and plotted as the percentage of the baseline TER (t = 0 h). Values are the average ± SD from a single representative experiment performed in triplicate. *B*, PMN were added to the basolateral aspect of inverted T84 monolayers cultured on 0.4-μm pore filters and fMLP was added to the lower chamber (PMN/fMLP). After 2 h, the samples were fixed, embedded, sliced, and visualized by light microscopy as described in *Materials and Methods.* PMN and epithelium are in contact by cellular processes extending between PMN and epithelial monolayers through the filter pores. Bar = 10 μm.

the decrease in TER in Fig. 3*A* was slower, taking ~4–6 h to fall to minimal levels.

PMN-stimulated, migration-independent decrease in monolayer TER does not appear to be due to a soluble factor but requires cell-cell contact

Based on the above results, we hypothesized that the observed PMN-stimulated, migration-independent decrease in TER might be due to a soluble factor released from activated PMN. However, as shown in Figs. 1*C* and 3*A*, when fMLP was added to the same reservoir that contained PMN at a concentration that strongly activates PMN (1 μM), no decrease in TER occurred, as would be expected if fMLP stimulated the release of a soluble factor. Furthermore, we observed no change in TER in monolayers treated with supernatants from samples with PMN-stimulated decreases in TER (PMN/fMLP, data not shown). The addition of protease inhibitors to the upper reservoir did not inhibit the drop in TER stimulated by PMN (data not shown), suggesting that the decrease in epithelial TER was not due to PMN proteases. Also, the addition of donor-matched serum (1% v/v) to the samples did not inhibit the decrease in TER. Serum has been shown to inhibit PMN β-defensins (31) and elastase (32), two PMN products shown to stimulate a decrease in epithelial barrier function.

To test whether the TER response was dependent on cell-cell contact, we placed an additional filter with 0.22-μm pores directly above the filter on which the epithelial monolayer was cultured. This configuration further separated PMN from epithelial cells by ~10–20 μm. This resulted in the ablation of the PMN-stimulated decrease in TER, potentially due to the lack of direct physical contact between PMN and epithelial cells.

We next processed samples for microscopic evaluation to determine whether PMN were able to contact the T84 monolayer across the 0.4-μm pore filters (Fig. 3*B*). As can be seen, numerous cellular processes are observed extending between adherent PMN and epithelial cells on the opposite side of the surface. Samples of epithelial monolayers cultured on filters for 7 days or PMN applied to filters with fMLP in the lower chamber demonstrated that both cell types extend cellular processes into the 0.4-μm pores (data not shown). These images suggest that PMN and epithelial cells are able to contact each other across 0.4-μm pore filters in the absence of transmigration and that the observed permeability changes are due to contact-dependent events.

Paracellular flux of small solutes is increased in PMN-stimulated monolayers

PMN-induced effects on epithelial barrier function were next examined by measuring the unidirectional diffusion of [^{14}C]-D-mannitol and FITC-dextran (3 kDa) across T84 monolayers cultured on 0.4-μm pore filters (Table II). Pretreatment of T84 monolayers with EDTA before the addition of [^{14}C]-D-mannitol or FITC-dextran to disrupt TJ was used as a positive flux control. As demonstrated in Table II, PMN-stimulated T84 monolayers show enhanced permeability to small solutes ([^{14}C]-D-mannitol) under conditions of inhibited transmigration. In addition, high-density PMN transmigration in the basolateral to apical direction across monolayers grown on 5-μm pore filters was used to evaluate enhanced flux as a result of transmigrating PMN. For both positive controls, an increase in [^{14}C]-D-mannitol and FITC-dextran flux

Table II. *Mannitol and dextran permeability across PMN-stimulated epithelial monolayers*[a]

Upper Reservoir/Lower Reservoir	[^{14}C]-D-Mannitol (cpm)	3-kDa FITC-Dextran (μg/ml)
Media/media[b]	285.7 ± 78.5	0.30 ± 0.08
PMN/media	404.3 ± 165.6	0.21 ± 0.14
PMN/fMLP (0.4 μm)	1,578.7 ± 1,158.7	0.40 ± 0.26
PMN/fMLP (5 μm)[b]	1,337.0 ± 401.49	1.01 ± 0.12
Media/fMLP	320.7 ± 139.5	0.22 ± 0.06
Media/EDTA[b,c]	18,492.3 ± 4,705.7	5.54 ± 6.15

[a] Data represent the average ± SD; values are from a single representative experiment done in triplicate. PMN were interacted with T84 inverted monolayers for 3 h at 37°C as described in *Materials and Methods.* At t = 0 h, [^{14}C]-D-mannitol (0.25 μCi) or FITC-dextran (1 mg/ml final concentration) was added to the basolateral reservoir (upper) and its appearance in the apical reservoir (lower) was measured at 3 h of incubation.

[b] T84 monolayer cultured on 5 μm pore filter.

[c] T84 monolayer treated with 2 mM EDTA in HBSS without calcium or magnesium.

was detected at 3 h and correlated with a decrease in epithelial TER (Table II). For samples in which PMN were added to the basolateral aspect of T84 monolayers cultured on small pore filters (0.4 μm), a migration-independent decrease in epithelial TER correlated with enhanced flux of small solutes ([^{14}C]-D-mannitol) but not larger molecules (3-kDa FITC-dextran). PMN-induced mannitol flux across T84 monolayers cultured on 0.4- and 5-μm pore filters was not significantly different at $t = 3$ h. While the flux of FITC-dextran was slightly increased in 0.4-μm pore filters under PMN/fMLP conditions, it was not significantly greater than that observed for the negative controls.

Transmigration-independent increase in epithelial paracellular permeability is not a result of gross changes in TJ architecture

Immunofluorescence microscopy experiments were performed to evaluate the TJ and adherens junction (AJ) for structural alterations secondary to PMN-stimulated changes in paracellular permeability. We stained monolayers with PMN-stimulated, migration-independent decreased TER for a comprehensive assortment of intercellular junction proteins, including occludin, ZO-1, ZO-2, JAM, claudin-1, -2, or -5, α- and β-catenin, E-cadherin, and α-actinin (Fig. 4, images shown only for occludin). As shown in Fig. 4, no alteration in occludin staining occurred for any condition tested (Media/Media, PMN/Media, and PMN/fMLP). Similarly, no changes in the staining profiles were observed for the other intercellular junction proteins listed above (data not shown). These results suggest that migration-independent changes in epithelial barrier function are not secondary to gross alterations in intercellular junctional structure.

We used confocal microscopy to examine TJ structure during uninhibited PMN migration across T84 monolayers cultured on 5-μm pore filters (Fig. 5). For these experiments, BCECF-AM-loaded PMN were stimulated to migrate across T84 monolayers in the basolateral to apical direction toward a gradient of fMLP for 15 min. After 15 min of transmigration, epithelial monolayers were stained with anti-ZO-1 Abs to visualize the TJ protein. Confocal en face (*x-y*) images were taken at the level of the TJ (Fig. 5*A*) and mid-epithelium (Fig. 5*B*), as depicted in the diagram shown in Fig. 5*D*. At 15 min, we observed that PMN migration across the epithelial monolayer occurred primarily as single cells (Fig. 5*B*). At later time points, migrating PMN formed clusters that result in the formation of epithelial wounds or discontinuities (21). Occasionally, PMN are seen emerging at the level of the TJ (Fig. 5*A*, *, *lower right corner*). However, the majority of migrating PMN are observed in the middle portion of the epithelium (Fig. 5*B*). In the corresponding reconstructed *x-z* image (Fig. 5*C*), PMN within the epithelium are in close proximity to the TJ (Fig. 5*C*, open arrows). As can be seen in the *x-z* image, staining of ZO-1 indicated that the TJ is in fact structurally intact immediately subjacent to migrating PMN. Together with the data in Fig. 4*B*, these findings argue that TJ disruption does occur, but only as a late event during PMN transepithelial migration.

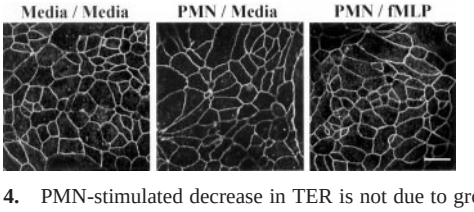

FIGURE 4. PMN-stimulated decrease in TER is not due to gross alteration in distribution of TJ proteins. En face confocal microscopy of T84 monolayers stained for occludin in PMN-stimulated monolayers. PMN were applied to the basolateral aspect of epithelial monolayers cultured on 0.4-μm pore supports and incubated at 37°C until the TER of PMN-stimulated condition (PMN/fMLP) had fallen to ~30% of baseline. Samples included medium only (Media/Media), PMN only (PMN/Media), and PMN with fMLP in the lower reservoir (PMN/fMLP). Bar = 20 μm.

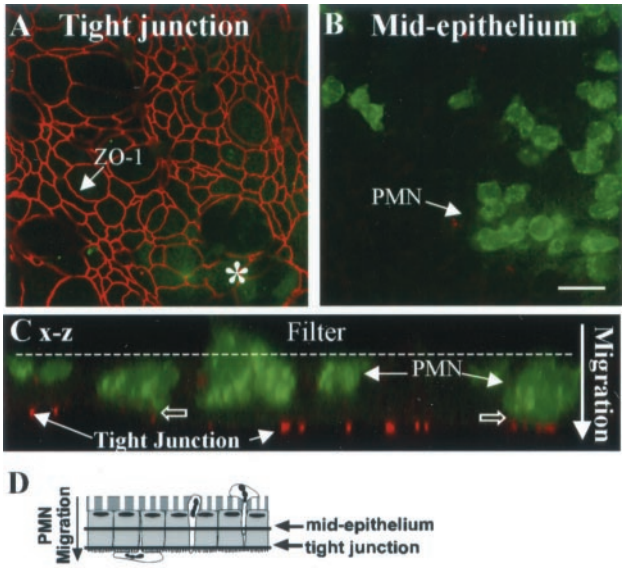

FIGURE 5. TJ protein staining remains the same after migrating PMN enter the paracellular space of epithelium. BCECF-AM-loaded PMN were induced to migrate across T84 monolayers in the basolateral to apical direction toward a gradient of fMLP. After 15 min of migration, samples were processed for immunofluorescence microscopy. *A*, Confocal en face image of epithelial monolayer stained for ZO-1 at the level of the TJ. ZO-1 staining demonstrates the typical "chicken wire" pattern of cell-cell junctions. Migrating PMN can be observed starting to emerge at the *lower right corner* of the image (*). *B*, Confocal en face image of BCECF-AM-labeled PMN within the same monolayers shown in *A*. *C*, Reconstructed *xz*-confocal image of the same monolayer shown in *A* and *B*. The filled arrow denotes the direction of PMN transmigration, and the filter that the epithelial monolayer is cultured on is identified by the dotted line. The open arrows identify areas in which PMN are in very close proximity to the TJ and demonstrate the preservation of TJ morphology presumably until just before the PMN movement across the TJ. *D*, Diagram of PMN transmigration through inverted epithelial monolayer indicating the position in the monolayer where confocal images were taken. Bar = 20 μm.

PMN stimulate changes in the actomyosin ring of T84 monolayers

Phosphorylation of the regulatory L chain of myosin II (MLC) has been shown to induce enhanced paracellular permeability of both epithelial (33, 34) and endothelial cells (26). We examined T84 monolayers with PMN migration-independent, stimulated enhanced permeability for changes in MLC. An increase in localization of MLC at the actomyosin ring was observed in PMN-stimulated samples (data not shown). Furthermore, Fig. 6*A* demonstrates enhanced phosphorylation of junction-associated MLC (pMLC) in PMN-stimulated samples. For these experiments, inverted monolayers cultured on 0.4-μm pore filters were interacted with PMN for 3 h at 37°C, followed by fixation and colabeling with rhodamine-phalloidin to visualize the actomyosin ring and an Ab that specifically recognizes only the phosphorylated form of MLC (pMLC) (Fig. 6*A*). Confocal en face images were then taken at the level of the actomyosin ring. A low level of pMLC was found at the actomyosin ring in medium and PMN control monolayers (Fig. 6*A*). In monolayers with PMN-stimulated, decreased barrier function (PMN/fMLP), a significant increase in staining intensity of pMLC is seen. These results indicate that an enhanced association of pMLC with

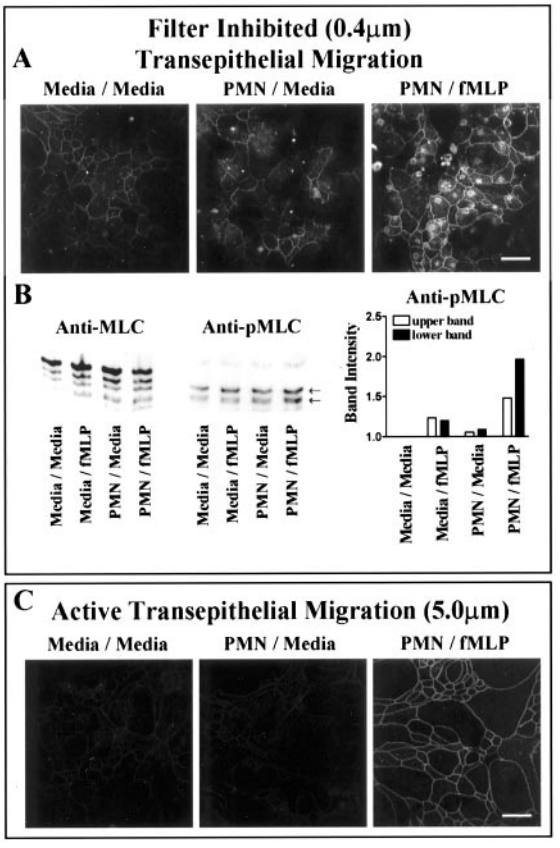

FIGURE 6. PMN-stimulated, transmigration-independent phosphorylation of epithelial MLC. *A* and *B*, Media or PMN were applied to the upper reservoir (basolateral aspect of T84 monolayers) cultured on 0.4-μm porous supports (0.4 μm) with or without fMLP in the lower reservoir. Samples were incubated at 37°C until the TER had fallen to ~30% of the baseline TER. En face confocal microscopy of T84 monolayers stained for phospho-MLC at the actomyosin ring (*A*) described in *Materials and Methods*. *B*, Western blot analysis of epithelial MLC in PMN-stimulated monolayers. Whole cell lysates of inverted T84 monolayers cultured on 0.4-μm pore filters that had been interacted with basolaterally applied PMN for 3 h at 37°C were run on urea-glycerol gels and Western blotted for MLC using either a goat anti-MLC Ab that recognizes both unphosphorylated and phosphorylated forms of both isoforms of MLC, or a rabbit anti-pMLC Ab that specifically recognizes the phosphorylated form of MLC. *Lane 1*, Media only (Media/Media); *lane 2*, fMLP only (Media/fMLP); *lane 3*, PMN only (PMN/Media) and PMN/fMLP. *Right panel*, Densitometry quantitation of pMLC bands (arrows). Each sample band is normalized to the respective medium control band. Bars are the average from two separate experiments. *C*, En face confocal microscopy of T84 monolayers with active PMN transepithelial migration in the basolateral to apical direction stained for pMLC at the actomyosin ring. Media or PMN were added to the upper reservoir (basolateral aspect) of T84 monolayers cultured on 5-μm porous supports with or without fMLP in the lower reservoir. After 15 min of PMN migration, samples were processed for immunofluorescence microscopy as described in *Materials and Methods*. Bar = 20 μm.

F-actin filaments accompanied the observed decrease in barrier function.

Samples were then prepared for biochemical analysis of MLC phosphorylation in PMN-stimulated monolayers. Due to the kinetics of the migration-independent, PMN-stimulated decrease in TER and the observed increase in MLC phosphorylation at 3 h by confocal microscopy, we prepared samples for analysis after 3 h of PMN stimulation. As shown in Fig. 6*B*, an increase in MLC phosphorylation was observed by Western blot analysis in monolayers with PMN-enhanced permeability. Fig. 6*B* demonstrates that T84 epithelial cells express two isoforms of MLC, each containing two phosphorylation sites (threonine 18 and serine 19). Therefore, anti-MLC recognizes up to six different protein bands (Fig. 6*B*, *left panel*) and anti-pMLC recognizes up to four bands (Fig. 6*B*, *right panel*). The band highlighted in Fig. 6*B* by the *lower arrow* is actually two bands that did not fully separate by electrophoresis. In monolayers with PMN-enhanced permeability (PMN/fMLP), an increase in MLC phosphorylation was observed when samples were probed with the pMLC-specific Ab (Fig. 6*B*, anti-pMLC, arrows). These results demonstrate that an increase in pMLC in epithelial monolayers correlates with PMN-stimulated enhanced permeability.

We next analyzed epithelial monolayers for similar changes in MLC phosphorylation under conditions of active PMN migration. Just as observed in samples with blocked PMN transmigration (Fig. 6*A*, PMN/fMLP), an increase in anti-pMLC staining was seen at the cell-cell junction (Fig. 6*C*). For these experiments PMN were allowed to migrate across T84 monolayers cultured on 5-μm pore filters in the basolateral to apical direction for 15 min. Samples were then fixed and stained with anti-pMLC Ab. Medium-only and PMN-only control monolayers demonstrated a low level of pMLC at the apical junction. Markedly enhanced phosphorylation of MLC at the apical junction was clearly observed throughout monolayers with actively migrating PMN (Fig. 6*C*). Because increased phosphorylation of MLC was also observed in T84 monolayers cultured on 0.4-μm pore filters with PMN-stimulated decrease in TER (Fig. 6*A*), these results indicate that increased phosphorylation of MLC occurs before the passage of migrating PMN through the epithelium. However, we observed that the level of MLC phosphorylation remained elevated throughout the monolayer, suggesting that there is a global increase in MLC phosphorylation. Alternatively, it is possible that an increase in MLC phosphorylation is observed in areas without PMN present as a consequence of PMN that had previously migrated through that area.

PMN-stimulated decrease in TER is accompanied by changes in epithelial protein phosphorylation at the level of the TJ

Previous studies have shown that changes in the phosphorylation state of TJ structural proteins results in modulation of paracellular permeability (35, 36). Therefore, monolayers with PMN-stimulated, migration-independent enhanced permeability were examined for changes in tyrosine phosphorylation at the level of the TJ by confocal microscopy (Fig. 7). In the medium control sample (Fig. 7*A*, Media/Media), anti-phosphotyrosine staining was observed at a low level in the cytoplasm and at the TJ. A slight increase in intensity of phosphotyrosine staining was observed in both the cytoplasm and TJ in the PMN control sample (Fig. 7*B*, PMN/Media), yet a significant increase in phosphotyrosine staining was observed in the cytoplasm and TJ in samples with PMN-stimulated enhanced paracellular permeability (Fig. 7*C*, PMN/fMLP). To distinguish changes at the TJ from those at the AJ, monolayers were also colabeled with anti-E-cadherin and anti-phosphotyrosine Abs. Unlike the enhanced tyrosine phosphorylation at the TJ observed in PMN-stimulated monolayers (PMN/fMLP), no change in the intensity of phosphotyrosine staining at the AJ was observed in PMN-stimulated monolayers compared with control monolayers (data not shown). Furthermore, these phosphorylation changes were distinct from those observed with MLC in Fig. 6, as MLC is phosphorylated only on serine and threonine residues. These results indicate that PMN stimulate changes in tyrosine phosphorylation specifically at the TJ and suggest that TJ phosphorylation occurs as an early event in the epithelial response to PMN transmigration.

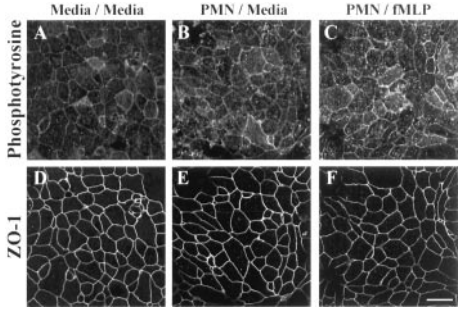

FIGURE 7. PMN-stimulated, transmigration-independent, enhanced tyrosine phosphorylation at the TJ. *A–C*, Confocal en face images of epithelial monolayers stained for phosphotyrosine proteins at the TJ. *D–F*, Corresponding images of the same monolayers stained for TJ protein ZO-1. PMN were applied to the basolateral aspect of T84 monolayers cultured as inverted monolayers on filters with 0.4-μm pores. Samples were incubated at 37°C until the TER of the experimental samples (*C* and *F*, PMN/fMLP) had fallen to ~30% of the baseline TER (t = 0 h). Samples included medium control (*A* and *D*, Media/Media), PMN control (*B* and *E*, PMN/Media), and PMN-stimulated monolayers (*C* and *F*, PMN/fMLP). Bar = 20 μm.

Next, we examined PMN-stimulated changes in protein tyrosine phosphorylation in monolayers at the level of the TJ during active PMN transepithelial migration. We observed a similar increase in TJ tyrosine phosphorylation in samples with actively migrating PMN but not in medium or PMN control samples (data not shown). A time course study was used to evaluate the increase in protein tyrosine phosphorylation during PMN migration (Fig. 8).

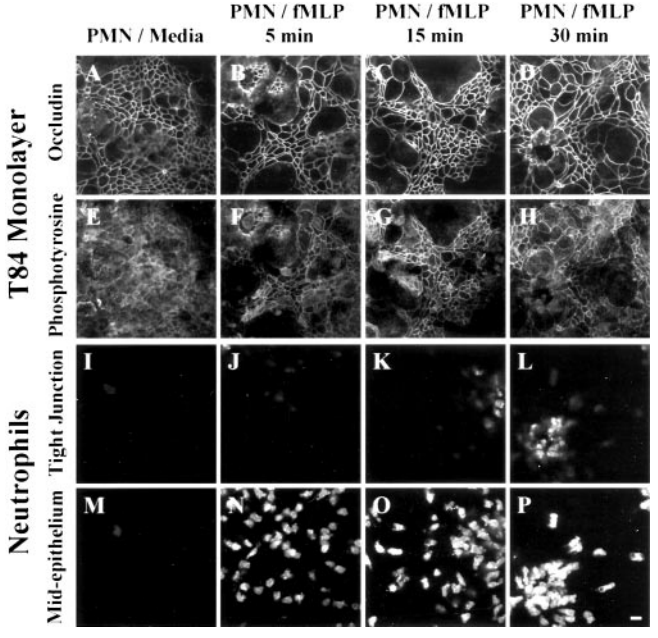

FIGURE 8. Time course of phosphotyrosine staining at the TJ during PMN transmigration. PMN were induced to migrate across T84 monolayers in the basolateral to apical direction toward a gradient of fMLP. At designated time points, samples were fixed and processed for confocal microscopy. *A–D*, En face images of epithelial monolayers stained for occludin. *E–H*, Corresponding images of epithelial monolayers stained for phosphotyrosine proteins at the same level as occludin. *I–P*, Corresponding images of the same monolayers in *A–D* of BCECF-AM-loaded PMN taken at the level of the TJ (*I–L*) and mid-monolayer level (*M–P*). Increasing intensity of phosphotyrosine staining was observed at the TJ with respect to time in epithelial monolayers with transmigrating PMN (*F–H*). Bar = 20 μm.

For these experiments, BCECF-AM-loaded PMN were allowed to migrate across T84 monolayers cultured on 5-μm pore filters in the basolateral to apical direction for 5, 15, and 30 min. Monolayers were colabeled with anti-occludin and anti-phosphotyrosine Abs. A confocal en face image was first captured at the level of the TJ by focusing on the staining of occludin (Fig. 8, *A–D*). A second set of images was captured of the tyrosine phosphorylation staining (Fig. 8, *E–H*). The confocal images are of a single plane of focus. The uneven height of the epithelial cells within the monolayers is because the monolayers are cultured on filters. At the magnification shown, it was extremely difficult to image a complete field in which all of the TJs were within the same plane of focus. To determine the position of migrating PMN within the monolayer with respect to the TJ, additional images were captured of the BCECF-AM-labeled PMN at the level of the TJ (Fig. 8, *I–L*) and mid-epithelium level (Fig. 8, *M–P*). As can be seen in Fig. 8, *E–H*, an increase in the intensity of phosphotyrosine staining at the TJ was observed with respect to time. At 5 min, large numbers of migrating PMN were found within the monolayer (Fig. 8*N*) but had not reached the level of the TJ (Fig. 8*J*). This result and results obtained with filter-inhibited migration indicate that increased protein tyrosine phosphorylation occurs before the passage of migrating PMN through the epithelium. These findings are consistent with the changes observed in MLC phosphorylation (see Fig. 6). Moreover, in support of this interpretation, we observed no further increase in phosphotyrosine staining from 15 to 30 min of PMN migration (Fig. 8, *G* and *H*). At 30 min of PMN migration, enhanced phosphotyrosine staining at the TJ was present throughout the monolayer even though PMN were primarily observed migrating across the monolayer in large clusters (Fig. 8, *O* and *P*), suggesting that migrating PMN may stimulate a global increase in protein tyrosine phosphorylation. However, it is also possible that increased protein tyrosine phosphorylation is a result of PMN that had previously migrated and it remains elevated due to the constant PMN migration throughout the entire monolayer.

PMN transmigration-dependent redistribution of serine-phosphorylated epithelial proteins from the cytoplasm to nucleus

Changes in the staining patterns of phosphoserine and phosphothreonine were also examined during both filter-inhibited and -uninhibited PMN transmigration. As described in Fig. 8, monolayers were fixed and stained with Abs that specifically recognize phosphoserine or phosphothreonine residues. No change in staining was observed for phosphoserine staining in samples with filter-inhibited PMN migration (data not shown). In addition, we did not consistently observe significant alterations in phosphothreonine staining in T84 monolayers with filter-inhibited or noninhibited PMN migration. However, dramatic alterations in the localization of phosphoserine proteins were observed in samples with uninhibited PMN transmigration (Fig. 9). For these experiments, BCECF-AM-loaded PMN were induced to migrate across T84 monolayers in the basolateral to apical direction. After 5, 15, and 30 min of PMN migration, the samples were fixed and stained with anti-phosphoserine Ab and propidium iodide to visualize the nuclei. While we did not see changes in serine phosphorylation at the TJ, a significant redistribution of cytoplasmic phosphoserine staining into the nucleus occurred (Fig. 9, *C–E*). After 5 min of PMN transmigration, colocalization of phosphoserine proteins with propidium iodide staining appeared to be throughout the monolayer (Fig. 9*C*). At later time points, 15 and 30 min (Fig. 9, *D* and *E*), colocalization of phosphoserine proteins and propidium iodide appeared to be restricted to the epithelial cells adjacent to transmigrating PMN. These results suggest that transmigration of PMN

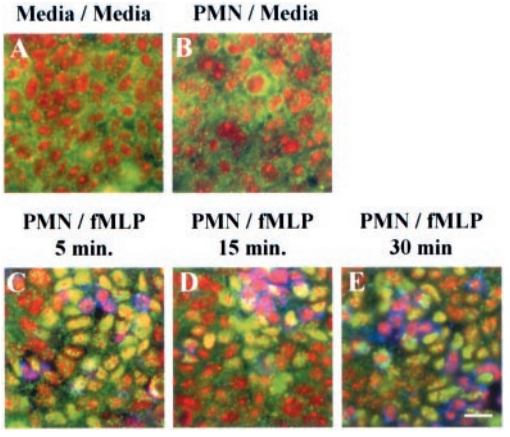

FIGURE 9. PMN migration through T84 monolayers stimulates relocalization of phosphoserine proteins into the nucleus. PMN were induced to migrate across T84 monolayers in the basolateral to apical direction toward a gradient of fMLP. After designated time points, monolayers were stained with propidium iodine (red) to localize nuclei, anti-phosphoserine Ab (green), and anti-CD18 Ab (blue) to localize migrating PMN. Confocal en face images were taken at the level of the epithelial nuclei. Control monolayers included medium only (*A*, Media/Media) and PMN only (*B*, PMN/Media). Shown is relocalization of epithelial phosphoserine proteins from the cytoplasm into the nucleus as PMN transmigrate across the monolayer. Initially, the relocalization of the observed phosphoserine proteins appeared to be a general occurrence throughout the monolayer (*C*, PMN/fMLP at 5 min) but at later time points was observed to be restricted to areas around the migrating PMN (*D* and *E*, PMN/fMLP at 15 and 30 min, respectively). Bar = 20 μm.

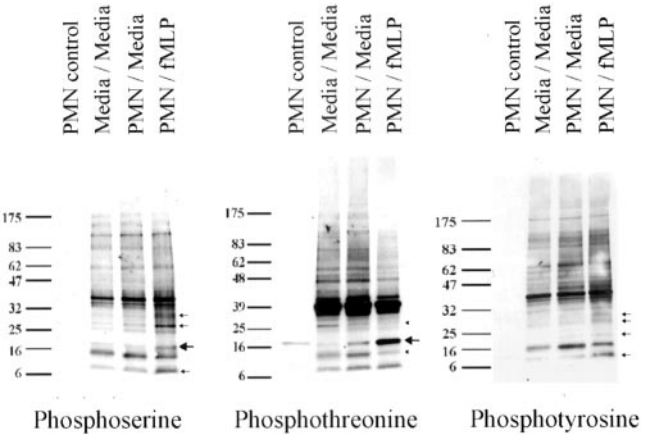

FIGURE 10. PMN-stimulated T84 monolayers display changes in phosphorylation of multiple proteins. PMN were induced to migrate across T84 monolayers in the basolateral to apical direction toward a gradient of fMLP. After 15 min of migration, whole cell lysates of epithelial monolayers were prepared in a urea buffer. Equal protein amounts of sample were run on a 4–20% gradient SDS-PAGE and Western blotted with anti-phosphoserine (*A*), anti-phosphothreonine (*B*), and anti-phosphotyrosine (*C*) Abs. Samples included cell lysate of 30% of the total number of PMN applied to T84 monolayers (PMN control), medium only (Media/Media), PMN only (PMN/Media), and transmigrating PMN (PMN/fMLP). Filled arrows indicate an increase in protein phosphorylation in the PMN/fMLP sample compared with control samples. Arrowheads indicate a decrease in protein phosphorylation in the PMN/fMLP sample compared with control samples. Larger filled arrows indicate that the 20-kDa protein band is MLC.

activates signaling cascades that result in relocalization of serine-phosphorylated proteins into the nucleus within adjacent epithelial cells.

Migrating PMN stimulate changes in epithelial protein phosphorylation

Given the immunofluorescence staining patterns of phosphoproteins in Figs. 7–9, we analyzed PMN-migrated monolayers by Western blot for changes in phosphorylation of specific protein bands. As seen in Fig. 10, changes in protein phosphorylation levels (serine, threonine, and tyrosine) were observed for multiple proteins. For these studies, whole cell lysates of T84 monolayers used for PMN transmigration assays were separated by SDS-PAGE, transferred to nitrocellulose, and probed with anti-phosphoserine-, anti-phosphothreonine-, and anti-phosphotyrosine-specific Abs (Fig. 10). Samples were run in triplicate and separately probed with the three types of anti-phosphoprotein Abs. Actin was used as a protein concentration loading control (data not shown). To control for contaminating PMN proteins, equivalent numbers of PMN as would be within such monolayers were analyzed in parallel. As can be seen in Fig. 10, several alterations in protein phosphorylation were observed as either increases (Fig. 10, arrows) or decreases (Fig. 10, arrowheads) in band intensity or appearance/loss of bands from monolayers with PMN transmigration as compared with control cell lysates. An increase in phosphoserine and threonine staining intensity was observed in a band at 20 kDa (Fig. 10, large arrow). Reprobing these Western blots with anti-MLC Ab confirmed that this protein was MLC (data not shown), further supporting previous experiments indicating that migrating PMN stimulate an increase in epithelial MLC phosphorylation. An increase in phosphoserine staining of proteins at ~28 and 30 kDa and an increase in phosphotyrosine staining of protein bands at ~10, 20, 30, and 35 kDa were also observed. Furthermore, a decrease in phosphothreonine staining of two proteins of 12 and 26 kDa was seen.

Discussion

Using a well-characterized in vitro model of PMN transepithelial migration, we have demonstrated that PMN initiate important signaling events in epithelial cells that result in altered paracellular permeability and protein phosphorylation at the level of the TJ and nucleus. We postulate that such PMN-stimulated epithelial signaling serves to coordinate PMN transmigration. Previous studies from our laboratory have shown that there is distinct polarity to the efficacy of PMN transepithelial migration. Specifically, PMN migration is more efficient (5- to 20-fold) in the basolateral to apical direction compared with the reverse (23). The mechanisms for this polarized response are not understood. In this study, we further demonstrate that signaling responses between PMN and epithelial cells occur in a polarized fashion that alters epithelial barrier function.

These findings suggest a two-step model of early and late events for PMN-stimulated changes in intestinal epithelial function during transepithelial migration. Early events include an increase in paracellular permeability to small solutes after subepithelial PMN are stimulated with a transepithelial gradient of the chemoattractant, fMLP. This effect is dependent upon PMN-epithelial cell contact but does not require transepithelial migration. Furthermore, early signaling events included migration-independent phosphorylation of intercellular junction-associated MLC and protein tyrosine phosphorylation at the level of the TJ. These epithelial changes were also observed during active PMN transepithelial migration, confirming that they are early components of this dynamic process. Analysis of epithelial lysates from monolayers during active PMN transepithelial migration confirmed alteration in phosphorylation of multiple proteins. Late events included redistribution of serine-phosphorylated proteins from cytoplasmic pools to

the nucleus in epithelial cells adjacent to migrating PMN. This observation suggests that later events in transepithelial migration may involve activation of epithelial nuclear transcription factors.

Substantial evidence has accumulated demonstrating that extravagating PMN play an active role in the alteration of endothelial barrier function. This is thought to result in facilitating the passage of PMN through the vasculature or blood brain barrier (4). While there are likely similarities between mechanisms of PMN-induced alteration of endothelial barrier function and epithelial barrier function observed in this work, our laboratory has previously shown that there are considerable differences between the process of PMN transendothelial migration and PMN transepithelial migration (19). For instance, while selectins (L-, P-, and E-selectins) play an important role in capturing and rolling PMN along the vascular endothelium during the initial stages of PMN attachment, they do not appear to play a role in PMN adhesion to epithelia (20). Second, even though CD11b/CD18 is required for firm adhesion of PMN to both epithelia and endothelia preceding migration (23), the endothelial ligand, ICAM-1, does not appear to be involved in PMN migration across intestinal epithelia (37). In fact, the epithelial counter receptor(s) for CD11b/CD18 are currently undefined. Despite the lack of evidence linking ICAM-1 to PMN transepithelial migration, there is evidence that ligation of endothelial ICAM-1 by migrating PMN results in activation of endothelial signaling cascades. In particular, Ab cross-linking or ligation by β_2 integrin of migrating lymphocytes in brain and vascular endothelium activates signaling pathways involved in regulation of the actin cytoskeleton, including intracellular calcium release (38–40) and activation of $p60^{src}$ (41), Rho (42, 43), and protein kinase C (44). This results in enhanced endothelial permeability and facilitation of transendothelial passage of PMN from the vasculature into the tissues (42, 45). Therefore, while ICAM-1 does not appear to play this role in intestinal epithelia, it is reasonable to assume that another basolaterally expressed ligand may play a related role during PMN transepithelial migration.

We have begun to investigate possible epithelial ligands involved in PMN-stimulated epithelial signaling. Due to the polarized nature of the response, such a ligand would be basolaterally expressed. The addition of inhibitory Abs to candidate proteins, including CD29, CD61, CD47, and CD44, had no effect on the PMN-stimulated decrease in TER in our assays (data not shown). On the PMN side, it is likely that the ligand is not CD11b/CD18 because anti-CD11b/CD18 Abs fail to inhibit the permeability response. Interestingly, CD18-independent adhesive events have been shown to play an important role in transepithelial migration in the lung (46). Indeed, we have observed that CD18-independent migration accounts for 5–10% of the total PMN migration in the basolateral to apical direction through intestinal epithelial monolayers (see Fig. 1).

PMN-activated signaling pathways in both endothelium and epithelium (as demonstrated in this work) result in changes in barrier function due to modification of the actin cytoskeleton by phosphorylation of MLC (47). Others have reported that phosphorylation of MLC can result from the activation of two separate signaling cascades, by Rho-associated kinase through the calcium-independent Rho effector pathway (48), and by MLC kinase (MLCK), a calcium/calmodulin-dependent kinase (49). During transendothelial migration, it has been shown that PMN can stimulate phosphorylation of MLC after adhesion to endothelial cells (50), and pharmacological inhibition of endothelial MLCK has been shown to result in decreased PMN transmigration (50). In intestinal epithelial cells, activation of protein kinase C, a serine/threonine kinase, results in increased TER through phosphorylation and inactivation of MLCK and hence decreased phosphorylation of MLC (51). Attempts to inhibit the PMN-induced decrease in TER with phosphorylation inhibitors have been inconclusive (data not shown). We believe this was due to the inherent problems of working with this two-cell system because these experiments required that the inhibitors be washed out before addition of PMN to avoid direct effects on PMN. In addition, some inhibitors resulted in direct effects on TER independent of PMN.

We also observed PMN-stimulated changes in generalized tyrosine phosphorylation at the level of the TJ before transepithelial migration that correlated with increased permeability. This finding is consistent with other inhibitor-based studies that demonstrated enhanced protein tyrosine phosphorylation at the TJ correlates with alterations in permeability (52, 53). For example, increased tyrosine phosphorylation of ZO-1 has been shown to result in enhanced paracellular permeability (52). We are currently investigating PMN-stimulated changes in phosphorylation of TJ proteins.

During active transepithelial migration, we observed redistribution of serine-phosphorylated proteins from cytoplasmic pools to the nucleus in epithelial cells adjacent to migrating PMN. Because this effect was not observed with inhibited PMN migration, it is clearly dependent on paracellular passage of PMN and thus occurs subsequent to phosphorylation of MLC and other TJ proteins. This translocation event is suggestive of PMN stimulation of an epithelial nuclear transcription factor(s). A potential candidate would be NF-κB. However, we have not observed relocalization of NF-κB subunit p65 from the cytoplasm to nucleus in epithelial cell during PMN transepithelial migration (data not shown). Studies are under way to identify specific epithelial proteins that are phosphorylated during PMN transepithelial migration. Further characterization of such PMN-stimulated effects on epithelial cells will improve our understanding of the role of migrating leukocytes on epithelial function and may provide new ideas for therapeutic manipulation of pathologic inflammation of mucosal surfaces.

Acknowledgments

We are grateful to Susan Voss and Mildred Pochet for their expert technical assistance. We are also grateful to Peter Goldberg for his assistance with urea glycerol gel analysis of MLC phosphorylation.

References

1. Fanning, A. S., L. L. Mitic, and J. M. Anderson. 1999. Transmembrane proteins in the tight junction barrier. *J. Am. Soc. Nephrol. 10:1337.*
2. Madara, J. L. 1998. Regulation of the movement of solutes across tight junctions. *Annu. Rev. Physiol. 60:143.*
3. Stevenson, B. R., and B. H. Keon. 1998. The tight junction: morphology to molecules. *Annu. Rev. Cell Dev. Biol. 14:89.*
4. Edens, H. A., and C. A. Parkos. 2000. Modulation of epithelial and endothelial paracellular permeability by leukocytes. *Adv. Drug Deliv. Rev. 41:315.*
5. Parkos, C. A. 1997. Molecular events in neutrophil transepithelial migration. *BioEssays 19:865.*
6. Irvine, E. J., and J. K. Marshall. 2000. Increased intestinal permeability precedes the onset of Crohn's disease in a subject with familial risk. *Gastroenterology 119:1740.*
7. Schmitz, H., C. Barmeyer, M. Fromm, N. Runkel, H. D. Foss, C. J. Bentzel, E. O. Riecken, and J. D. Schulzke. 1999. Altered tight junction structure contributes to the impaired epithelial barrier function in ulcerative colitis. *Gastroenterology 116:301.*
8. Madara, J. L., and J. Stafford. 1989. Interferon-γ directly affects barrier function of cultured intestinal epithelial monolayers. *J. Clin. Invest. 83:724.*
9. Nishiyama, R., T. Sakaguchi, T. Kinugasa, X. Gu, R. P. MacDermott, D. K. Podolsky, and H. C. Reinecker. 2001. IL-2 receptor β subunit dependent and independent regulation of intestinal epithelial tight junctions. *J. Biol. Chem. 276:35571.*
10. Nusrat, A., C. von Eichel-Streiber, J. R. Turner, P. Verkade, J. L. Madara, and C. A. Parkos. 2001. *Clostridium difficile* toxins disrupt epithelial barrier function by altering membrane microdomain localization of tight junction proteins. *Infect. Immun. 69:1329.*
11. Tafazoli, F., C. Q. Zeng, M. K. Estes, K. E. Magnusson, and L. Svensson. 2001. NSP4 enterotoxin of rotavirus induces paracellular leakage in polarized epithelial cells. *J. Virol. 75:1540.*
12. Clarke, H., A. P. Soler, and J. M. Mullin. 2000. Protein kinase C activation leads to dephosphorylation of occludin and tight junction permeability increase in LLC-PK1 epithelial cell sheets. *J. Cell Sci. 113:3187.*

13. Simonovic, I., J. Rosenberg, A. Koutsouris, and G. Hecht. 2000. Enteropathogenic *Escherichia coli* dephosphorylates and dissociates occludin from intestinal epithelial tight junctions. *Cell. Microbiol. 2:305.*
14. Tsukamoto, T., and S. K. Nigam. 1999. Role of tyrosine phosphorylation in the reassembly of occludin and other tight junction proteins. *Am. J. Physiol. 276: F737.*
15. Farshori, P., and B. Kachar. 1999. Redistribution and phosphorylation of occludin during opening and resealing of tight junctions in cultured epithelial cells. *J. Membr. Biol. 170:147.*
16. Bresnick, A. R. 1999. Molecular mechanisms of nonmuscle myosin-II regulation. *Curr. Opin. Cell Biol. 11:26.*
17. Turner, J. R. 2000. "Putting the squeeze" on the tight junction: understanding cytoskeletal regulation. *Semin. Cell Dev. Biol. 11:301.*
18. Nash, S., J. Stafford, and J. L. Madara. 1987. Effects of polymorphonuclear leukocyte transmigration on the barrier function of cultured intestinal epithelial monolayers. *J. Clin. Invest. 80:1104.*
19. Parkos, C. A., S. P. Colgan, and J. L. Madara. 1994. Interactions of neutrophils with epithelial cells: lessons from the intestine. *J. Am. Soc. Nephrol. 2:138.*
20. Parkos, C. A., S. P. Colgan, C. Delp, M. A. Arnaout, and J. L. Madara. 1992. Neutrophil migration across a cultured epithelial monolayer elicits a biphasic resistance response representing sequential effects on transcellular and paracellular pathways. *J. Cell Biol. 117:757.*
21. Nusrat, A., C. A. Parkos, T. W. Liang, D. K. Carnes, and J. L. Madara. 1997. Neutrophil migration across model intestinal epithelia: monolayer disruption and subsequent events in epithelial repair. *Gastroenterology 113:1489.*
22. Parsons, P. E., K. Sugahara, G. R. Cott, R. J. Mason, and P. M. Henson. 1987. The effect of neutrophil migration of prolonged neutrophil contact on epithelial permeability. *Am. J. Pathol. 129:302.*
23. Parkos, C. A., C. Delp, M. A. Arnaout, and J. L. Madara. 1991. Neutrophil migration across a cultured intestinal epithelium: dependence on a CD11b/CD18-mediated event and enhanced efficiency in the physiologic direction. *J. Clin. Invest. 88:1605.*
24. Cereijido, M., and D. D. Sabatini. 1978. Polarized monolayers formed by epithelial cells on a permeable and translucent support. *J. Cell Biol. 77:853.*
25. Madara, J. L., S. P. Colgan, A. Nusrat, C. Delp, and C. A. Parkos. 1992. A simple approach to measurement of electrical parameters of cultured epithelial monolayers: use in assessing neutrophil-epithelial interactions. *J. Tissue Cult. Methods 14:209.*
26. Garcia, J. G. N., H. W. Davis, and C. E. Patterson. 1995. Regulation of endothelial cell gap formation and barrier dysfunction: role of myosin light chain phosphorylation. *J. Cell Physiol. 163:510.*
27. Persechini, A., K. E. Kamm, and J. T. Stull. 1986. Different phosphorylated forms of myosin in contracting tracheal smooth muscle. *J. Biol. Chem. 261:6293.*
28. Verin, A. D., C. E. Patterson, M. A. Day, and J. G. Garcia. 1995. Regulation of endothelial cell gap formation and barrier function by myosin-associated phosphatase activities. *Am. J. Physiol. 269:L99.*
29. Sanders, S. E., J. L. Madara, D. McGuirk, D. S. Gelman, and S. P. Colgan. 1995. Assessment of inflammatory events in epithelial permeability: a rapid screening method using fluorescein dextrans. *Epithelial Cell Biol. 4:25.*
30. Nash, S., J. Stafford, and J. L. Madara. 1988. The selective and superoxide-independent disruption of intestinal epithelial tight junctions during leukocyte transmigration. *Lab. Invest. 59:531.*
31. Nygaard, S. D., T. Ganz, and M. W. Peterson. 1993. Defensins reduce the barrier integrity of a cultured epithelial monolayer without cytotoxicity. *Am. J. Respir. Cell Mol. Biol. 8:193.*
32. Peterson, M. W., M. E. Walter, and S. D. Nygaard. 1995. Effect of neutrophil mediators on epithelial permeability. *Am. J. Respir. Cell Mol. Biol. 13:719.*
33. Turner, J. R., B. K. Rill, S. L. Carlson, D. Carnes, R. Kerner, R. J. Mrsny, and J. L. Madara. 1997. Physiological regulation of epithelial tight junctions is associated with myosin light-chain phosphorylation. *Am. J. Physiol. 273:C1378.*
34. Hecht, G., L. Pestic, G. Nikcevic, A. Koutsouris, J. Tripuraneni, D. D. Lorimer, G. Nowak, V. Guerriero, Jr., E. L. Elson, and P. D. Lanerolle. 1996. Expression of the catalytic domain of myosin light chain kinase increases paracellular permeability. *Am. J. Physiol. 271:C1678.*
35. Hirase, T., S. Kawashima, E. Y. Wong, T. Ueyama, Y. Rikitake, S. Tsukita, M. Yokoyama, and J. M. Staddon. 2001. Regulation of tight junction permeability and occludin phosphorylation by Rhoa-p160ROCK-dependent and -independent mechanisms. *J. Biol. Chem. 276:10423.*
36. Nusrat, A., C. A. Parkos, P. Verkade, C. S. Foley, T. W. Liang, W. Innis-Whitehouse, K. K. Eastburn, and J. L. Madara. 2000. Tight junctions are membrane microdomains. *J. Cell Sci. 113:1771.*
37. Parkos, C. A., S. P. Colgan, M. S. Diamond, A. Nusrat, T. W. Liang, T. A. Springer, and J. L. Madara. 1996. Expression and polarization of intercellular adhesion molecule-1 on human intestinal epithelia: consequences for CD11b/CD18-mediated interactions with neutrophils. *Mol. Med. 2:489.*
38. Huang, A. J., J. E. Manning, T. M. Bandak, M. C. Ratau, K. R. Hanser, and S. C. Silverstein. 1993. Endothelial cell cytosolic free calcium regulates neutrophil migration across monolayers of endothelial cells. *J. Cell Biol. 120:1371.*
39. Furie, M. B., B. L. Naprstek, and S. C. Silverstein. 1987. Migration of neutrophils across monolayers of cultured microvascular endothelial cells: an in vitro model of leukocyte extravasation. *J. Cell Sci. 88:161.*
40. Su, W.-H., H. Chen, J. Huang, and C. J. Jen. 2000. Endothelial $[Ca^{2+}]_i$ signaling during transmigration of polymorphonuclear leukocytes. *Blood 96:3816.*
41. Durieu-Trautmann, O., N. Chaverot, S. Cazaubon, A. D. Strosberg, and P. O. Couraud. 1994. Intercellular adhesion molecule 1 activation induces tyrosine phosphorylation of the cytoskeleton-associated protein cortactin in brain microvessel endothelial cells. *J. Biol. Chem. 269:12536.*
42. Adamson, P. A., S. Etienne, P.-O. Couraud, V. Calder, and J. Greenwood. 1999. Lymphocyte migration through brain endothelial cell monolayers involves signaling through endothelial ICAM-1 via a Rho-dependent pathway. *J. Immunol. 162:2964.*
43. Etienne, S., P. Adamson, J. Greenwood, A. D. Strosberg, S. Cazaubon, and P. O. Couraud. 1998. ICAM-1 signaling pathways associated with Rho activation in microvascular brain endothelial cells. *J. Immunol. 161:5755.*
44. Etienne-Manneville, S., J. B. Manneville, P. Adamson, B. Wilbourn, J. Greenwood, and P. O. Couraud. 2000. ICAM-1-coupled cytoskeletal rearrangements and transendothelial lymphocyte migration involve intracellular calcium signaling in brain endothelial cell lines. *J. Immunol. 165:3375.*
45. Wójciak-Stothard, B., L. Williams, and A. J. Ridley. 1999. Monocyte adhesion and spreading on human endothelial cells is dependent on Rho-regulated receptor clustering. *J. Cell Biol. 145:1293.*
46. Mizgerd, J. P., H. Kubo, G. J. Kutkoski, S. D. Bhagwan, K. Scharffetter-Kochanek, A. L. Beaudet, and C. M. Doerschuk. 1997. Neutrophil emigration in the skin, lungs, and peritoneum: different requirements for CD11/CD18 revealed by CD18-deficient mice. *J. Exp. Med. 186:1357.*
47. Hixenbaugh, E. A., Z. M. Goeckeler, N. N. Papaiya, R. B. Wysolmerski, S. C. Silverstein, and A. J. Huang. 1997. Stimulated neutrophils induce myosin light chain phosphorylation and isometric tension in endothelial cells. *Am. J. Physiol. 273:H981.*
48. Maekawa, M., T. Ishizaki, S. Boku, N. Watanabe, A. Fujita, A. Iwamatsu, T. Obinata, K. Ohashi, K. Mizuno, and S. Narumiya. 1999. Signaling from Rho to the actin cytoskeleton through protein kinases ROCK and LIM-kinase. *Science 285:895.*
49. Fukata, Y., M. Amano, and K. Kaibuchi. 2001. Rho-Rho-kinase pathway in smooth muscle contraction and cytoskeletal reorganization of non-muscle cells. *Trends Pharmacol. Sci. 22:32.*
50. Saito, H., Y. Minamiya, M. Kitamura, S. Saito, K. Enomoto, K. Terada, and M. Ogawa. 1998. Endothelial myosin light chain kinase regulates neutrophil migration across human umbilical vein endothelial cell monolayer. *J. Immunol. 161:1533.*
51. Turner, J. R., J. M. Angle, E. D. Black, J. L. Joyal, D. B. Sacks, and J. L. Madara. 1999. PKC-dependent regulation of transepithelial resistance: roles of MLC and MLC kinase. *Am. J. Physiol. 277:C554.*
52. Staddon, J. M., K. Herrenknecht, C. Smales, and L. L. Rubin. 1995. Evidence that tyrosine phosphorylation may increase tight junction permeability. *J. Cell Sci. 108:609.*
53. Antonetti, D. A., A. J. Barber, L. A. Hollinger, E. B. Wolpert, and T. W. Gardner. 1999. Vascular endothelial growth factor induces rapid phosphorylation of tight junction proteins occludin and zonula occluden 1: a potential mechanism for vascular permeability in diabetic retinopathy and tumors. *J. Biol. Chem. 274: 23463.*
54. Berglund, J. J., M. Riegler, Y. Zolotarevsky, E. Wenzl, and J. R. Turner. 2001. Transmucosal resistance and myosin regulatory light chain phosphorylation are regulated by Na^+-glucose cotransport in human jejunum. *Am. J. Physiol. 281:G1487.*